Robust Time-Varying Synthesis Load Modeling in Distribution Networks Considering Voltage Disturbances

Mingjian Cui, *Senior Member, IEEE*, Jianhui Wang, *Senior Member, IEEE*, Yishen Wang, Ruisheng Diao, *Senior Member, IEEE*, and Di Shi, *Senior Member, IEEE*

***Abstract*—Uncertain power sources are increasingly integrated into distribution networks and causing more challenges for the traditional load modeling. A variety of distributed load components present dynamic characteristics with time-varying parameters. Toward this end, this paper proposes a robust time-varying parameter identification (TVPI) method for synthesis load modeling (SLM) in distribution networks, including time-varying ZIP, induction motor, and equivalent impedance models. The nonlinear optimization model is developed and solved by the nonlinear least square (NLS) to find the minimum error between estimated outputs and measurements. To cope with TVPI deteriorated by voltage disturbances, dynamic programming is first used to detect the disturbance. Then, a robust TVPI engine is designed to constrain the estimated time-varying parameters within a stable range. Furthermore, advanced tolerance thresholds are also required during iterations of NLS. Numerical simulations on the 9- and 129-bus distribution systems verify the effectiveness and robustness of the proposed TVPI method. Also, this method can be robust to the ambient noise of measurements.**

***Index Terms*—Composite load modeling, distribution network, dynamic programming, synthesis load modeling.**

NOMENCLATURE

A. Acronyms:

CLM	Composite load modeling.
IM	Induction motor.
MAPE	Mean absolute percentage error.
NLS	Nonlinear least square.
PDF	Probability density function.
RMSE	Root mean square error.
SLM	Synthesis load modeling.
TVPI	Time-varying parameter identification.

B. Parameter and State Variables:

$a_{p,t}, b_{p,t}, c_{p,t}$	Percentages for ZIP active power at t.
$a_{q,t}, b_{q,t}, c_{q,t}$	Percentages for ZIP reactive power at t.
$V_{CLM,t}, V_{SLM,t}$	CLM and SLM voltage magnitude at t.
V_0	Nominal voltage magnitude.
$P_{ZIP,t}, Q_{ZIP,t}$	Active and reactive power of ZIP load at t.
$v'_{d,t}, v'_{q,t}$	d- and q-axis transient voltage at t.
$R_{r,t}, R_{s,t}$	Rotor and stator resistance at t.
$X_{r,t}, X_{s,t}$	Rotor and stator reactance at t.
$X_{m,t}, X'_t$	Magnetizing and short circuit reactance at t.
$i_{d,t}, i_{q,t}$	d- and q-axis stator current at t.
s_t	Rotor slip at t.
H_t	Inertia constant of induction motor at t.
$u_{d,t}, u_{q,t}$	d- and q-axis bus voltage at t.
$P_{IM,t}, Q_{IM,t}$	Active and reactive power of IM load at t.
$P_{CLM,t}, Q_{CLM,t}$	Total active and reactive power of CLM at t.
$\lambda_{p,t}, \lambda_{q,t}$	Proportions of ZIP load in total active and reactive power of CLM at t.
$P_{SLM,t}, Q_{SLM,t}$	Total active and reactive power of SLM at t.
$R_{l,t}, X_{l,t}$	Resistance and reactance of equivalent impedance at t.
P_t, Q_t, V_t	Measured active power, reactive power, and voltage at t.
η_1, η_2	Thresholds of the basic and robust TVPI.
t, T	Index of time point and its total number.
$S(\cdot), J(\cdot)$	Score function and objective function.
$R(\cdot)$	Disturbance rule defined by users.
A_m, s_m, e_m	The mth detected disturbance with its start-time s_m and end-time e_m.
M	Total number of detected disturbances.

C. Sets, Vectors, Matrices, and Functions:

$\boldsymbol{\tau}_t, \boldsymbol{\varsigma}_t, \boldsymbol{\xi}_t$	Sets of CLM bus voltage, IM state, and time-varying SLM parameter variables at time t.
$\boldsymbol{\varepsilon}_{\boldsymbol{\xi},t}, \boldsymbol{\varepsilon}_{\mathbf{f},t}, \boldsymbol{\varepsilon}_{\mathbf{h},t}$	Sets of process nioses at time t.
$\mathbf{f}(\cdot), \mathbf{h}(\cdot)$	Generalized nonlinear function vectors of state transition and measurement equations.
$\mathbf{g}(\cdot)$	Generalized matrix model of time-varying SLM.
$\boldsymbol{\varsigma}_{t\|t-1}, \boldsymbol{\xi}_{t\|t-1}$	IM state and SLM parameter variables at time t estimated by time t-1.
$\boldsymbol{\tau}_{t-1}, \boldsymbol{\varsigma}_{t-1}, \boldsymbol{\xi}_{t-1}$	Estimated CLM bus voltage, IM state, and SLM parameter variables at time t-1.
$\mathbf{Y}_t, \mathbf{X}_t, \tilde{\mathbf{X}}_t$	Sets of generalized output, input, and estimation at time t.
$\mathbf{X}_{t,i}$	Estimation at time t during the ith iteration.
$\boldsymbol{\varsigma}_{\mathrm{N}}, \boldsymbol{\xi}_{\mathrm{N}}$	Mean values of IM state and SLM parameter variables under historical normal operating conditions learned by users.

I. INTRODUCTION

TIME-varying load modeling is becoming more and more important due to the increasing integration of uncertain power resources into distribution networks. The impacts of time-varying load on power system stability, such as the voltage stability, have been drawing the attention of worldwide

M. Cui and J. Wang are with the Department of Electrical and Computer Engineering, Southern Methodist University, Dallas, TX, 75275 USA (e-mail: {mingjiancui, jianhui}@smu.edu).

Y. Wang, R. Diao, and D. Shi are with GEIRI North America, San Jose, CA, 95134 USA (e-mail: {yishen.wang, ruisheng.diao, di.shi}@geirina.net).

Manuscript received, 2018.

researchers and engineers [1]–[3]. In North America, the development of load modeling by the Western Electricity Coordinating Council (WECC) has been a significant effort in the passing years [4].

In the common transmission system, the load modeling structures consist of static model, dynamic model, and composite model. The composite load modeling (CLM) with specific parameters has been widely used since it considers both the static and the dynamic characteristics of the static model and dynamic model [5], [6]. The CLM model in the transmission system is mainly used to characterize the dynamics of electrical load [7]. In the distribution networks, the SLM model can estimate the load more accurately than the conventional CLM model. This is because the SLM model includes not only the common CLM model but also the equivalent impedance which cannot be neglected in the distribution network. By just considering the CLM part, the effect of the distribution network cannot be characterized properly [8]. Theoretically, the equivalent impedance of load modeling cannot be ignored due to its relatively high network losses caused by the low voltage in distribution networks.

To identify load parameters, both statistical and heuristic techniques have been widely explored in the existing literature. For statistical techniques, Hiskens [9] used the nonlinear least-square based method to estimate parameters by the best fit between measurements and model response. Zhao *et al*. [10] utilized the maximum likelihood approach to estimate parameters for power system state dynamics. Kock *et al*. [11] used the gradient method to estimate parameters of the induction motor (IM). For heuristic techniques, neural networks [12], [13] were used to describe the complicated dynamic behavior of load modeling. The simulated annealing algorithm [14] was used to find the global optimum for identifying load parameters. However, most of these algorithms do not consider the time-varying characteristics of load parameters. Due to the frequent changes caused by uncertain power resources, it is highly necessary to develop a method to estimate time-varying parameters for load modeling in distribution networks [2]. Ignoring the time-varying characteristics of dynamic SLM can lead to erroneous results in the transient stability studies of distribution system operations. This is to say, the estimated parameters at the current time point are not only related with the current measurements (e.g., bus voltage, active power, and reactive power) but also dependent on the previous parameters of dynamic SLM in distribution networks.

Recently, time-varying load modeling has been focused on by worldwide researchers [15]. For example, Wang *et al*. [2] proposed a robust time-varying parameter identification technique for CLM in a batch-model regression form. Hung *et al*. [16] developed time-varying load models to determine the photovoltaic penetration level in a distribution network. Wang *et al*. [17] developed a time-varying exponential load model to assess conservation voltage reduction effects. However, all the aforementioned methods identify time-varying parameters only for the combined model of ZIP and IM (CLM model) rather than the combined model of ZIP, IM, and equivalent impedance (SLM model). In addition, few of these methods consider the impacts of voltage disturbances, which means that the robustness of these methods is still undetermined for operators. Here we define the term of "robustness" as the accuracy and stability of estimated parameters when voltage disturbances occur. Though measurement outliers are analyzed in [2], it is still performed in the transmission-level system and does not consider the equivalent impedance of SLM. Moreover, the impacts of different measurement noises on estimated time-varying parameters are not considered and analyzed.

For the transmission-level system, much research has been performed considering the specific application scenario. Hill [18] proposed a dynamic load model that is able to capture the usual nonlinear steady-state load behavior plus load recovery and overshoot. Ma *et al*. [19] investigated the possibility of reducing the number of composite load model parameters to be identified from field measurements. Han *et al*. [20] proposed the expectation-based composite load model to predict unseen data and provided methods for load bus classification and parameter identification. Choi *et al*. [21] addressed the issue of multiple local optimal solutions and the plateau problem in developing load models which are linked to the local identifiability problem. Bai *et al*. [22] combined the genetic algorithm and the nonlinear Levenberg-Marquardt algorithm to identify parameters for the aggregate load model. Ge *et al*. [23] presented a new event-oriented method of online load modeling for a microgrid based on synchrophasor data produced by phasor measurement units. Kim *et al*. [24] proposed a computationally efficient technique for estimating the composite load model parameters based on analytical similarity of parameter sensitivity. Wang *et al*. [25] proposed a parameter identification technique for composite ZIP and electronic loads by leveraging the support vector machine (SVM) approach.

For the distribution-level system, to the best of our knowledge, the time-varying SLM has not been studied previously for load modeling. Currently, the research of the existing demand response opportunities in the distribution networks, such as distributed energy resources, renewable energy, electric vehicle charging, home and building energy management [26], [27], is making load model parameters change more frequently in the time domain, which results in more time-varying parameters. It is imperative to understand the time-varying characteristics of loads for distribution system analysis and control. In addition, disturbances in measurements, such as the transient stability events, may deteriorate estimated results of time-varying parameters. Thus, it is highly needed to find a way to enhance the robustness of time-varying parameter estimation methods. To bridge the gap in the time-varying parameter identification (TVPI) of the SLM model, we seek to address three critical questions for distribution network operators. Is it possible to update the existing time-varying CLM with an equivalent impedance for distribution networks? How can we improve the accuracy of estimated time-varying parameters to be more stable to voltage disturbances? Can the estimated parameters be robust to different ambient measurement noises? To this end, this paper proposes a novel robust TVPI method for SLM in distribution networks. The SLM model can achieve better trade-off between the model accuracy

and estimation efficiency.

To distinguish our main contributions and differences from the existing literature, Table I compares a variety of load models and attributes that are discussed in several representative references. As shown in this table, most of the conventional load modeling research focuses on the CLM model (ZIP+IM) [5], [6], [19]–[24] and SLM model (ZIP+IM+Equivalent Impedance) [7], [8], [28] while neglecting its time-varying and robust attributes. Though these attributes are considered in [2], [15], [25], the equivalent impedance is still neglected due to the transmission-level simulation. In addition, impacts of measurement noises are not analyzed. Unlike the aforementioned literature, we for the first time propose an SLM model considering its time-varying and robust attributes. The main contributions of this paper include:

(i) A time-varying SLM for the TVPI of dynamic load modeling is constituted. The time-varying voltage drop on the equivalent impedance is decomposed into a real component and a reactive component. The total active and reactive power of SLM are formulated based on the active and reactive power of CLM and equivalent impedance. The time-varying SLM bus voltage is calculated using the time-varying CLM bus voltage and voltage drop on the equivalent impedance.

(ii) A method for identifying disturbances is developed. Dynamic programming is used to detect disturbances that violate rules defined by users. Smaller step- and function-tolerances are separately set for time points deteriorated by voltage disturbances to guarantee more reliable parameter identification results.

(iii) An effective robust engine is designed to cope with voltage disturbances and inserted into the time-varying SLM to enhance its robustness against disturbances. A learning-based method using mean values of time-varying parameters under historical normal operating conditions is formulated as an equality constraint in the developed robust TVPI engine.

The organization of this paper is as follows. In Section II, the time-varying SLM consisting of static load, induction motor (IM), and equivalent impedance is briefly introduced. Section III presents the detailed methodology of disturbance detection and its application for designing the robust TVPI engine. Case studies and result analysis performed on two simulated distribution networks are discussed in Section IV. Concluding remarks are summarized in Section VI.

II. Time-Varying Parameter Identification

Theoretically, load modeling is defined as a mathematical representation of the relationship between a bus voltage magnitude and the active/reactive power into the bus load [18]. Thus, it is assumed that only voltage magnitude, active power, and reactive power can be measured by operators in this paper.

A. Time-Varying ZIP Model

One of the typical static load model is the ZIP model, which mainly consists of three parts. The first part is the constant impedance (Z) component. The second part is the constant current (I) component. The third part is the constant power (P) component. Percentages of three components are assumed to be time-varying due to weather conditions or customer behaviors. The ZIP model is mathematically formulated by:

$$P_{ZIP,t} = a_{p,t}\left(V_{CLM,t}/V_0\right)^2 + b_{p,t}\left(V_{CLM,t}/V_0\right) + c_{p,t}, \quad (1)$$

$$Q_{ZIP,t} = a_{q,t}\left(V_{CLM,t}/V_0\right)^2 + b_{q,t}\left(V_{CLM,t}/V_0\right) + c_{q,t}, \quad (2)$$

where percentage parameters satisfy $a_{p,t}+b_{p,t}+c_{p,t}=1$ and $a_{q,t}+b_{q,t}+c_{q,t}=1$ at any time period t.

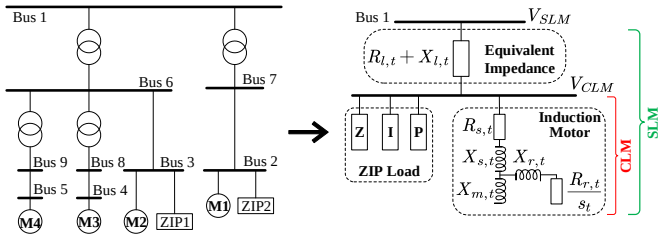

(a) 9-Bus Distribution System (b) SLM in Distribution Systems

Fig. 1. Equivalent circuit of SLM consisting of equivalent impedance, ZIP, and IM model: an example of 9-bus distribution system.

B. Time-Varying IM Model

The dynamic IM models are defined with a similar approach to the synchronous machine. In this paper, the typical squirrel-cage rotor model is used by additionally considering the time-varying impacts of customer behaviors. The simplified electrical circuit used for the squirrel-cage induction motor is shown in Fig. 1. The differential algebraic equations of state variables are formulated by:

$$\frac{dv'_{d,t}}{dt} = \frac{-R_{r,t}}{X_{r,t}+X_{m,t}}\left(v'_{d,t} + \frac{X^2_{m,t}}{X_{r,t}+X_{m,t}} i_{q,t}\right) + s_t v'_{q,t}, \quad (3)$$

$$\frac{dv'_{q,t}}{dt} = \frac{-R_{r,t}}{X_{r,t}+X_{m,t}}\left(v'_{q,t} - \frac{X^2_{m,t}}{X_{r,t}+X_{m,t}} i_{d,t}\right) - s_t v'_{d,t}, \quad (4)$$

$$\frac{ds_t}{dt} = \frac{1}{2H_t}\left[T_{m0}\left(1-s_t\right)^2 - v'_{d,t}i_{d,t} - v'_{q,t}i_{q,t}\right], \quad (5)$$

where the d-axis stator current $i_{d,t}$ and the q-axis stator current $i_{q,t}$ are given by:

$$i_{d,t} = \frac{R_{s,t}\left(u_{d,t}-v'_{d,t}\right) + X'_t\left(u_{q,t}-v'_{q,t}\right)}{R^2_{s,t}+X'^2_t}, \quad (6)$$

$$i_{q,t} = \frac{R_{s,t}\left(u_{q,t}-v'_{q,t}\right) - X'_t\left(u_{d,t}-v'_{d,t}\right)}{R^2_{s,t}+X'^2_t}, \quad (7)$$

where the quadratic sum of the d- and q-axis CLM bus voltages $u_{d,t}$ and $u_{q,t}$ should be equal to the square of the CLM bus voltage, given by:

$$V^2_{CLM,t} = u^2_{d,t} + u^2_{q,t}. \quad (8)$$

The short circuit reactance X'_t is formulated by:

$$X'_t = X_{s,t} + (X_{m,t}X_{r,t})/(X_{m,t}+X_{r,t}). \quad (9)$$

TABLE I
COMPARISON OF THIS PAPER WITH EXISTING LITERATURE

References	Models			Attributes		Operation System	Impacts of Measurement Noise
	ZIP	IM	Equivalent Impedance	Time-varying	Robust		
[5], [6], [19]–[24]	✘	✘	–	–	–	Transmission-Level	–
[7], [8]	✘	✘	✘	–	–	Distribution-Level	–
[15], [25]	✘	–	–	✘	✘	Transmission-Level	–
[2]	✘	✘	–	✘	✘	Transmission-Level	–
Research in this paper	✘	✘	✘	✘	✘	Distribution-Level	✘

The active and reactive power of the IM model can be formulated by using the states, time-varying parameters, and bus voltage variables, given by:

$$P_{IM,t} = \big[R_{s,t}\big(u_{d,t}^2 + u_{q,t}^2 - u_{d,t}v'_{d,t} - u_{q,t}v'_{q,t}\big) - X'_t\left(u_{d,t}v'_{q,t} - u_{q,t}v'_{d,t}\right)\big]/\Big(R_{s,t}^2 + X_t'^2\Big), \tag{10}$$

$$Q_{IM,t} = \big[X'_t\big(u_{d,t}^2 + u_{q,t}^2 - u_{d,t}v'_{d,t} - u_{q,t}v'_{q,t}\big) - R_{s,t}\left(u_{d,t}v'_{q,t} - u_{q,t}v'_{d,t}\right)\big]/\Big(R_{s,t}^2 + X_t'^2\Big). \tag{11}$$

More detailed information about the time-varying ZIP and IM models can be found in [2]. In the following section, we will introduce more details about the proposed time-varying SLM model. To the best of our knowledge, the time-varying SLM has not been studied previously for load modeling in the distribution-level system.

C. Time-Varying SLM

Based on models (1)–(2) and (10)–(11), the active and reactive power of the time-varying composite ZIP and IM model can be formulated by:

$$P_{CLM,t} = \lambda_{p,t}P_{ZIP,t} + (1-\lambda_{p,t})P_{IM,t}, \tag{12}$$

$$Q_{CLM,t} = \lambda_{q,t}Q_{ZIP,t} + (1-\lambda_{q,t})Q_{IM,t}. \tag{13}$$

With the active and reactive power of CLM and equivalent impedance, the total active and reactive power of SLM can be formulated as:

$$P_{SLM,t} = P_{CLM,t} + R_{l,t}\left(P_{CLM,t}^2 + Q_{CLM,t}^2\right)/V_{CLM,t}^2, \tag{14}$$

$$Q_{SLM,t} = Q_{CLM,t} + X_{l,t}\left(P_{CLM,t}^2 + Q_{CLM,t}^2\right)/V_{CLM,t}^2. \tag{15}$$

Given that the voltage drop on the equivalent impedance denoted as V_l, its real component ΔV_l and reactive component δV_l can be formulated as:

$$\Delta V_{l,t} = \left(P_{CLM,t}R_{l,t} + Q_{CLM,t}X_{l,t}\right)/V_{CLM,t}, \tag{16}$$

$$\delta V_{l,t} = \left(P_{CLM,t}X_{l,t} - Q_{CLM,t}R_{l,t}\right)/V_{CLM,t}. \tag{17}$$

Thus, the SLM bus voltage is given by:

$$V_{SLM,t} = \sqrt{\left(V_{CLM,t} + \Delta V_{l,t}\right)^2 + \left(\delta V_{l,t}\right)^2}. \tag{18}$$

D. TVPI Modeling and Solving

Assuming that the set of CLM bus voltage variables $\boldsymbol{\tau}_t = [u_{d,t}, u_{q,t}]$ and the set of IM state variables $\boldsymbol{\varsigma}_t = [v'_{d,t}, v'_{q,t}, s_t]$, the set of time-varying parameter variables of SLM can be denoted as:

$$\begin{aligned}\boldsymbol{\xi}_t = [&R_{s,t}, X_{s,t}, X_{m,t}, R_{r,t}, X_{r,t}, H_t, a_{p,t}, b_{p,t},\\ &a_{q,t}, b_{q,t}, \lambda_{p,t}, \lambda_{q,t}, R_{l,t}, X_{l,t}].\end{aligned} \tag{19}$$

Normally, values of time-varying parameter variables fluctuate slightly within a short time period. Thus, the relationship between adjacent time intervals can be expressed as:

$$\boldsymbol{\xi}_t = \boldsymbol{\xi}_{t-1} + \boldsymbol{\varepsilon}_{\boldsymbol{\xi},t}. \tag{20}$$

Based on (3)–(8) and (19), discrete state transitions and parameter transitions can be generalized as:

$$[\boldsymbol{\varsigma}_t, \boldsymbol{\xi}_t] = \mathbf{f}\left(\boldsymbol{\varsigma}_{t-1}, \boldsymbol{\xi}_{t-1}, \boldsymbol{\tau}_{t-1}\right) + \boldsymbol{\varepsilon}_{\mathbf{f},t}. \tag{21}$$

Based on (1), (2), and (9)–(18), the measurements equation can be generalized as:

$$[P_t, Q_t, V_t] = \mathbf{h}\left(\boldsymbol{\varsigma}_t, \boldsymbol{\xi}_t, \boldsymbol{\tau}_t\right) + \boldsymbol{\varepsilon}_{\mathbf{h},t}. \tag{22}$$

By integrating (20)–(22) to the matrix form, we can get:

$$\begin{bmatrix} \left[\boldsymbol{\varsigma}_{t|t-1}, \boldsymbol{\xi}_{t|t-1}\right] \\ [P_t, Q_t, V_t] \end{bmatrix} = \begin{bmatrix} [\boldsymbol{\varsigma}_t, \boldsymbol{\xi}_t] \\ \mathbf{h}\left(\boldsymbol{\varsigma}_t, \boldsymbol{\xi}_t, \boldsymbol{\tau}_t\right) \end{bmatrix} + \begin{bmatrix} \boldsymbol{\varepsilon}_{\mathbf{f},t} \\ \boldsymbol{\varepsilon}_{\mathbf{h},t} \end{bmatrix}, \tag{23}$$

where $\boldsymbol{\varsigma}_{t|t-1}$ and $\boldsymbol{\xi}_{t|t-1}$ can be approximately estimated by (21) and given by:

$$\left[\boldsymbol{\varsigma}_{t|t-1}, \boldsymbol{\xi}_{t|t-1}\right] \approx \mathbf{f}\left(\boldsymbol{\varsigma}_{t-1}, \boldsymbol{\xi}_{t-1}, \boldsymbol{\tau}_{t-1}\right). \tag{24}$$

Finally, we can get the generalized mathematical model of the time-varying SLM in distribution networks, given by:

$$\mathbf{Y}_t = \mathbf{g}\left(\mathbf{X}_t\right) + \boldsymbol{\varepsilon}_t, \tag{25}$$

where $\mathbf{X}_t = [\boldsymbol{\xi}_t, \boldsymbol{\varsigma}_t, \boldsymbol{\tau}_t]$, $\mathbf{Y}_t = \left[\boldsymbol{\varsigma}_{t|t-1}, \boldsymbol{\xi}_{t|t-1}, P_t, Q_t, V_t\right]$, and $\boldsymbol{\varepsilon}_t = [\boldsymbol{\varepsilon}_{\mathbf{f},t}, \boldsymbol{\varepsilon}_{\mathbf{h},t}]$.

Since measurement errors are not known beforehand in this paper, the weighted least square (WLS) method is not capable of solving the aforementioned model. Thus, the nonlinear least square (NLS) method is used to find the minimum error between estimated outputs and measurements. The objective function is given by:

$$\tilde{\mathbf{X}}_t = \arg\ \min_{\mathbf{X}_t}\left[\mathbf{Y}_t - \mathbf{g}\left(\mathbf{X}_t\right)\right]^{\mathrm{T}} \cdot \left[\mathbf{Y}_t - \mathbf{g}\left(\mathbf{X}_t\right)\right]. \tag{26}$$

To solve the nonlinear optimization problem in (26), the NLS method with the trust-region-reflective algorithm [29]

is chosen. This is because the developed nonlinear model of equations is not underdetermined and bound constraints need to be handled. The number of iterations of the developed nonlinear optimization problem depends on the solver's stopping criteria. For each time step t, the step-tolerance $|\mathbf{X}_{t,i}-\mathbf{X}_{t,i+1}|$ and function-tolerance $|\mathbf{g}(\mathbf{X}_{t,i})-\mathbf{g}(\mathbf{X}_{t,i+1})|$ should be smaller than the threshold η_1, given by:

$$\max\left[|\mathbf{X}_{t,i}-\mathbf{X}_{t,i+1}|, |\mathbf{g}(\mathbf{X}_{t,i})-\mathbf{g}(\mathbf{X}_{t,i+1})|\right]<\eta_1, \quad (27)$$

where i is the index of the ith iteration in the process of NLS.

III. Disturbances Detection and Robust Processing

Though time-varying parameters can be estimated by minimizing the objective function in (26), this aforementioned model only considers the impacts of system noise that is added into measurement variables and estimated in time-varying parameter variables. However, this model is still operated under normal stable conditions. When voltage disturbances occur, such as the slight voltage drop/rise, it will result in the corruption of other measurement variables (active and reactive power) and correspondingly deteriorate estimated TVPI results. Thus, in this section, a disturbance detection method is first described and two estimation methods, including our proposed robust TVPI method, are then proposed to handle TVPI estimation with voltage disturbances based on the time-varying model formulated in (23).

A. Dynamic Programming Based Disturbance Detection

Many methods have been used for disturbance detection, such as the wavelet decomposition [30], empirical mode decomposition [31], and principal components analysis [32]. However, these methods just transfer the measurements data in the time domain to other domains (such as the frequency domain). It is still very challenging to detect the exact start- and end-time of one disturbance using the aforementioned methods. To precisely insert the robust TVPI engine proposed in the following section, it is highly needed to use dynamic programming to obtain the exact start- and end-time of one disturbance beforehand [33]. Motivated by this need, a dynamic programming-based disturbance detection method is briefly introduced in this section.

Dynamic programming is a method for solving a complex problem by breaking it down into a collection of simpler subproblems [34]. It is used to combine adjacent intervals and detect disturbances with the maximum score function. First, adjacent intervals with the same ramping direction are rewarded by a score function if disturbance rules are satisfied; otherwise, the score rewarded is zero. This score function S is designed based on the length of intervals. Given a time interval (i,j) of discrete time points of measurement data and a time point k into this interval $(i<k<j)$, the score function presented in [35] is adopted and given by:

$$S(i,j)=(i-j)^2\times R(i,j), \quad (28)$$

where $R(i,j)$ represents the disturbance rules defined by users. In this paper, the disturbance rule is defined as a proportion

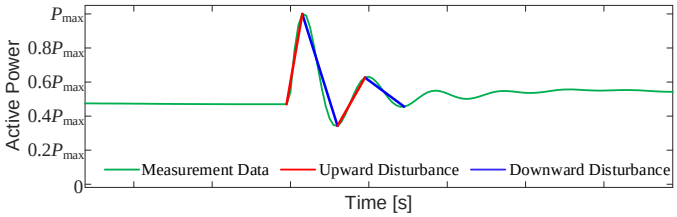

Fig. 2. An example of disturbances detected for active power.

of the maximum of one measurement variable. Taking active power as an example, the disturbance rule is defined as:

$$R(i,j)=\begin{cases}1, & \text{if } R(i,j)\geq\gamma P_{\max}\\ 0, & \text{if } R(i,j)<\gamma P_{\max}\end{cases}, \quad (29)$$

where γ is the proportion of the maximum active power and defined as γ=10% in this paper. Note that this proportion coefficient γ can be adjusted based on the user's preferences. For a better illustration, an example of the detected disturbance for active power is shown in Fig. 2. Then, an objective function J is constituted according to the dynamic programming, given by:

$$J(i,j)=\max_{i<k<j}[S(i,k)+J(k+1,j)]. \quad (30)$$

For the mth combined interval of a disturbance, i.e. $A_m=(s_m,e_m)$ with the start-time s_m and end-time e_m, the objective function using dynamic programming can be recursively expressed as:

$$\begin{aligned}J(s_m,e_m)&=\max_{s_m<k_1<e_m}S(s_m,k_1)+J(k_1+1,e_m)\\&=\max_{s_m<k_1<e_m}S(s_m,k_1)+\max_{k_1+1<k_2<e_m}S(k_1+1,k_2)\\&+\cdots+\max_{k_{i-1}+1<k_i<e_m}S(k_{i-1}+1,k_i)+J(k_i+1,e_m)\\&=\max_{s_m<k_1<k_2<\cdots<k_{i-1}<k_i<e_m}S(s_m,k_1)+S(k_1+1,k_2)\\&+\cdots+S(k_{i-1}+1,k_i)+S(k_i+1,e_m).\end{aligned} \quad (31)$$

The final detected disturbances of measurement data can be solved as:

$$J^*(\overline{s_1},\overline{e_M})=\sum_{m=1}^{M}S(s_m,e_m), \quad (32)$$

where M is the total number of detected disturbances in measurement data.

For any time point that is deteriorated by voltage disturbances $k\in A_m$, i.e., $\forall k: s_m<k<e_m$, one of estimation methods is proposed to consider higher precision of iterations. For any time point k, the step-tolerance $|\mathbf{X}_{t,i}-\mathbf{X}_{t,i+1}|$ and function-tolerance $|\mathbf{g}(\mathbf{X}_{t,i})-\mathbf{g}(\mathbf{X}_{t,i+1})|$ should be smaller than the threshold η_2.

$$\begin{cases}\max\left[\begin{array}{c}|\mathbf{X}_{k,i}-\mathbf{X}_{k,i+1}|\\|\mathbf{g}(\mathbf{X}_{k,i})-\mathbf{g}(\mathbf{X}_{k,i+1})|\end{array}\right]<\eta_1, & k\notin A_m\\ \max\left[\begin{array}{c}|\mathbf{X}_{k,i}-\mathbf{X}_{k,i+1}|\\|\mathbf{g}(\mathbf{X}_{k,i})-\mathbf{g}(\mathbf{X}_{k,i+1})|\end{array}\right]<\eta_2, & k\in A_m\end{cases}, \quad (33)$$

where η_2 is set to be significantly smaller than η_1, i.e., $\eta_2\ll\eta_1$, in order to get more reliable TVPI results.

B. Robust TVPI Engine Using Detected Disturbances

The estimated variables $\boldsymbol{\varsigma}_{t-1}$ and $\boldsymbol{\xi}_{t-1}$ at time t-1 in (24) may be deteriorated by the detected voltage disturbance information. Under this circumstance, the current estimated variables $\boldsymbol{\varsigma}_t$ and $\boldsymbol{\xi}_t$ at time t which are highly dependent on those at time t-1 would also be compromised in turn. To avoid this, we propose a learning-based method by inserting an equality constraint as a robust TVPI engine. It is assumed that mean values of time-varying parameters $\boldsymbol{\varsigma}_{\mathrm{N}}$ and $\boldsymbol{\xi}_{\mathrm{N}}$ under historical normal operating conditions have already been learned and known by users. From the perspective of the physical property of SLM, estimated parameters must be stabilized into a small range especially when voltage disturbances occur. Thus, the proposed robust TVPI engine requests that estimated variables are highly constrained by those under normal operating conditions.

For each time point k that is located into the detected interval of disturbance $k \in A_m$, i.e., $\forall k : s_m < k < e_m$, the time-varying model in (23) and (26) can be updated as:

$$\begin{cases} \begin{bmatrix} \boldsymbol{\varsigma}_{\mathrm{N}}, \boldsymbol{\xi}_{\mathrm{N}} \\ \left[\boldsymbol{\varsigma}_{k|k-1}, \boldsymbol{\xi}_{k|k-1}\right] \\ [P_k, Q_k, V_k] \end{bmatrix} = \begin{bmatrix} [\boldsymbol{\varsigma}_k, \boldsymbol{\xi}_k] \\ [\boldsymbol{\varsigma}_k, \boldsymbol{\xi}_k] \\ \mathbf{h}\left(\boldsymbol{\varsigma}_k, \boldsymbol{\xi}_k, \boldsymbol{\tau}_k\right) \end{bmatrix} + \begin{bmatrix} \varepsilon_{\mathrm{N},k} \\ \varepsilon_{\mathbf{f},k} \\ \varepsilon_{\mathbf{h},k} \end{bmatrix} \\ \max \begin{bmatrix} |\mathbf{X}_{k,i} - \mathbf{X}_{k,i+1}| \\ |\mathbf{g}\left(\mathbf{X}_{k,i}\right) - \mathbf{g}\left(\mathbf{X}_{k,i+1}\right)| \end{bmatrix} < \eta_1, \ k \notin A_m \\ \max \begin{bmatrix} |\mathbf{X}_{k,i} - \mathbf{X}_{k,i+1}| \\ |\mathbf{g}\left(\mathbf{X}_{k,i}\right) - \mathbf{g}\left(\mathbf{X}_{k,i+1}\right)| \end{bmatrix} < \eta_2, \ k \in A_m \end{cases} . \tag{34}$$

The overall framework of the proposed robust TVPI model for distribution networks is illustrated in Fig. 3, which mainly consists of three major steps: optimization modeling for measurements and disturbance detection, basic TVPI using NLS under normal operating conditions, and robust TVPI engine with smaller iteration threshold. These steps are described as follows:

- ***Step 1***: Based on the measurement data and time-varying SLM model of ZIP, IM, and equivalent impedance, the objective function of an optimization problem is developed (see Section II). Meanwhile, disturbances are detected based on the measurement data by using dynamic programming (see Section III-A).
- ***Step 2***: For each time point under normal operating conditions, the basic TVPI method is developed for the time-varying SLM in ***Step 1*** without considering too much computation of iterations when using NLS (see Section II-D).
- ***Step 3***: For each time point with a disturbance, a robust TVPI engine is designed and inserted into the basic TVPI method in ***Step 2***. More iterations are required by setting advanced tolerances to obtain robust TVPI results (see Section III-B).

IV. Case Studies

To evaluate the performance of the proposed robust methodology, two case studies are simulated on the 9- (see Fig. 1a) and 129-bus (see Fig. 4) distribution networks, respectively. There are 4 IM-load and 2 ZIP-load in the 9-bus system,

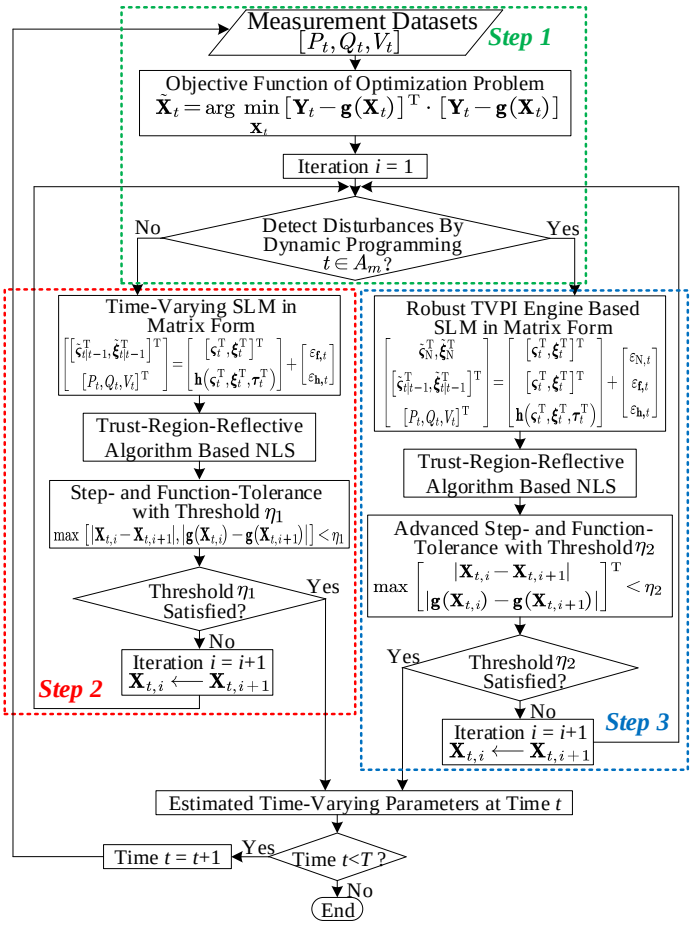

Fig. 3. Framework of the developed robust TVPI methodology for distribution networks.

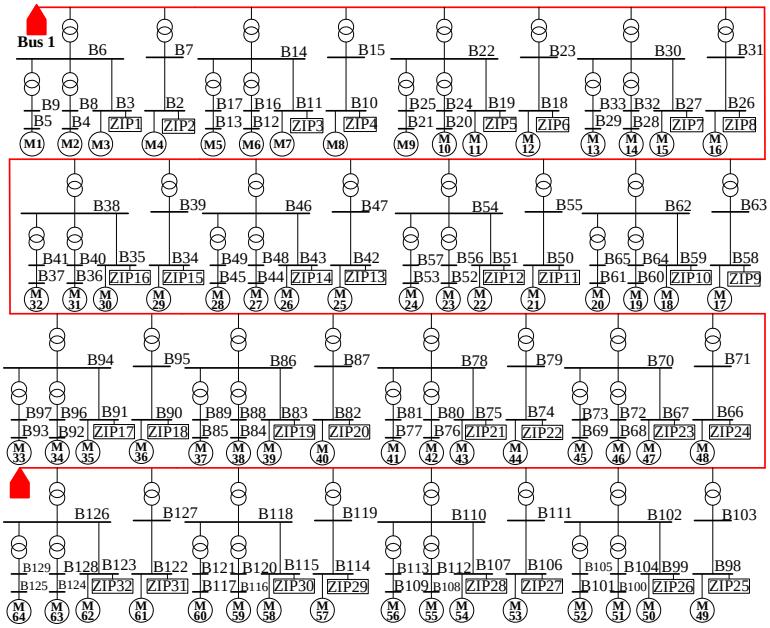

Fig. 4. Topology of the 129-bus distribution system.

and 64 IM-load and 32 ZIP-load in the 129-bus system. Note that a positive-sequence component is assumed and

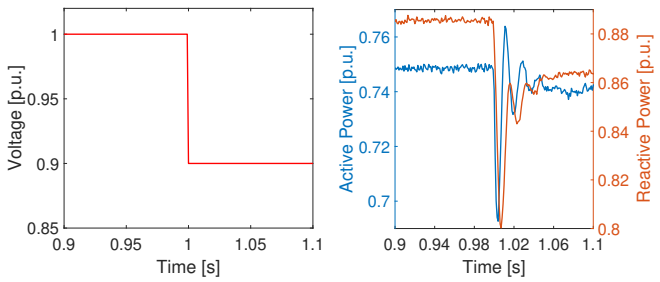

(a) Voltage data (b) Active and reactive power data

Fig. 5. Measurement data of active power, reactive power, and voltage in the 129-bus system.

modeled for both 9- and 129-bus distribution systems in this paper. The negative-sequence and zero-sequence components are not considered in the current simulation platform. For both distribution systems, we testify the effectiveness of the proposed method by comparing with two other methods:

- **Method 1:** basic TVPI using the model in (23) and constrained by (27).
- **Method 2:** TVPI considering disturbances using the model in (23) and constraints in (33).
- **Method 3 (*proposed*):** robust TVPI considering disturbances using the model and constraints in (34).

In the 9-bus distribution system, the SLM is compared with CLM to verify its effectiveness. In the 129-bus distribution system, the robustness of the proposed method is analyzed with different measurement noises. To mimic the real measurements with time-varying load changes, the simulated active power, reactive power, and voltage are added by a Gaussian noise with zero mean and a standard deviation as one thousandth of the corresponding value. The NLS solver lsqnonlin in MATLAB [29] is used to solve the aforementioned methods. Thresholds η_1 and η_2 of the stopping tolerance are set as 10^{-3} and 10^{-5}, respectively. For both distribution systems, a disturbance of voltage drop on the bus (Bus 1) connected with the main grid is set at 1 second. Measurement data of active power, reactive power, and voltage are assumed to be monitored and gathered at Bus 1 for both 9- and 129-bus systems. The bus voltage drops from 1 p.u. to 0.9 p.u. For the simplicity of illustration, the measurement data of active power, reactive power, and voltage in the 129-bus system is shown in Fig. 5.

To compare the robustness of different TVPI methods, three basic assumptions are made in this section:

(i) Historical mean values $\boldsymbol{\varsigma}_{\mathrm{N}}$ and $\boldsymbol{\xi}_{\mathrm{N}}$ of TVPI under normal operating conditions are assumed as the targeted benchmark values, which have been learned already and known by users in advance.

(ii) Estimated parameters are with less fluctuations under voltage disturbances. This assumption aims to guarantee the stability of TVPI values.

(iii) Estimated parameters are with smaller deviation from the historical mean value under normal operating conditions. This assumption aims to guarantee the accuracy of TVPI values.

Numerical metrics are used to evaluate the performance of different methods based on the estimated time-varying parameters. By comparing with mean values $\boldsymbol{\xi}_{\mathrm{N}}$ of actual time-varying parameters under historical normal operating conditions, mean absolute percentage error (MAPE) and root mean square error (RMSE) metrics are formulated as:

$$\mathrm{MAPE} = \frac{1}{T}\sum_{t=1}^{T} \left|\left(\boldsymbol{\xi}_t - \boldsymbol{\xi}_{\mathrm{N}}\right)/\boldsymbol{\xi}_t\right|, \tag{35}$$

$$\mathrm{RMSE} = \sqrt{\frac{1}{T}\sum_{t=1}^{T} \left(\boldsymbol{\xi}_t - \boldsymbol{\xi}_{\mathrm{N}}\right)^2}. \tag{36}$$

A. 9-Bus Distribution Network

1) Effectiveness Analysis of Estimated Parameters: Fig. 6 shows six representative parameters: $R_{s,t}$, $X_{s,t}$, $X_{r,t}$, $a_{p,t}$, $b_{p,t}$, and $a_{q,t}$, which are estimated by three methods. For the simplicity of comparison, the mean values of parameters under historical normal operating conditions (the blue solid line) are used as the benchmark. We define the robustness as not only the accuracy of estimated parameters but also the stability when voltage disturbances occur. As can be seen, the performance of Method 1 (the blue dash line) and Method 2 (the green dash line) is not stable and accurate compared with the benchmark mean value. A significant variation can be seen when using Method 1 and Method 2 which is caused by the voltage drop at 1 s. This is because both Method 1 and Method 2 only use the basic TVPI model where the current TVPI is highly dependent on that at the previous time point. Correspondingly, the estimation results are significantly misled by voltage disturbances. For most parameter curves, Method 1 shows the worst performance with the largest variation and the farthest distance to the blue solid line. By using the advanced tolerance threshold when disturbances occur, dash green parameter curves using Method 2 move closer to the blue solid line. However, there are still some time points with the most inaccurate results, such as parts of curves in Figs. 6a, 6d, and 6f (marked by black dash circles).

The red solid curves using the proposed Method 3 show the best performance compared with Method 1 and Method 2 with the closest distance to the blue solid line. Especially when disturbances occur at 1 second, Method 3 shows the most stable results with a slightest variation. This is because Method 3 uses the proposed robust TVPI engine which makes variables highly constrained by the normal operating TVPI.

To quantitatively evaluate the performance of Method 3, Table II illustrates the metrics of time-varying parameters using estimation methods, including MAPE, RMSE, and standard deviation. Method 3 shows the smallest metrics of parameters compared with Method 1 and Method 2. Theoretically, smaller MAPE and RMSE mean that using Method 3 can obtain more accurate results, while smaller standard deviations mean that using Method 3 can obtain more stable results with the least effects of voltage disturbances. These numerical results can obtain the same conclusion as in Fig. 6.

2) Effectiveness Analysis of Estimated Measurements: Fig. 7 shows the probability density function (PDF) of estimation errors of active and reactive power using time-varying

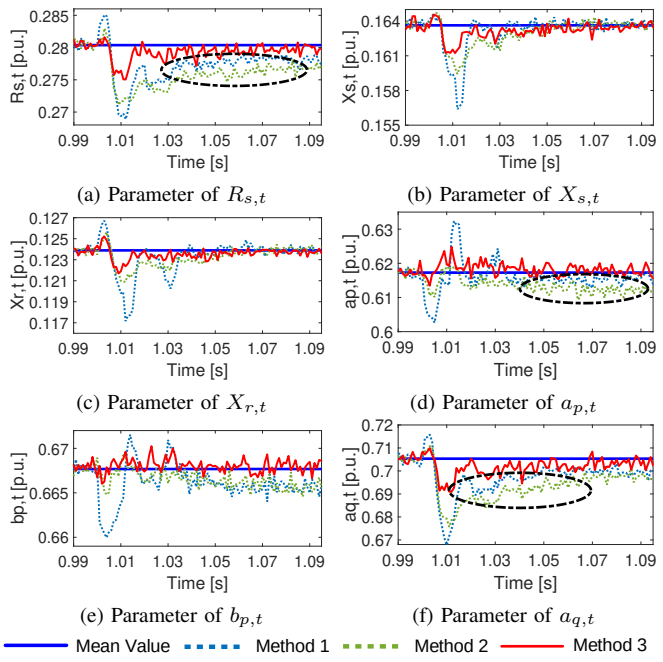

(a) Parameter of $R_{s,t}$ (b) Parameter of $X_{s,t}$

(c) Parameter of $X_{r,t}$ (d) Parameter of $a_{p,t}$

(e) Parameter of $b_{p,t}$ (f) Parameter of $a_{q,t}$

Fig. 6. Six representative parameters estimated in the 9-bus system.

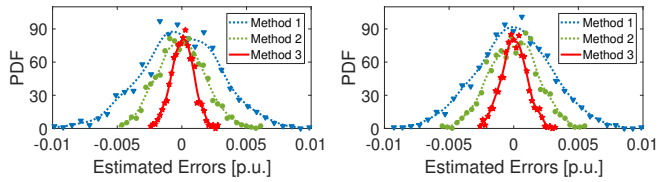

(a) Active Power (b) Reactive Power

Fig. 7. Errors of estimated active and reactive power in the 9-bus system.

parameters identified by different methods. As can be seen, Method 3 shows the smallest range (-0.003∼0.003) of estimation errors for both active and reactive power. Method 1 and Method 2 estimate the relatively larger ranges of errors with -0.01∼0.01 and -0.005∼0.005, respectively. This observation of estimated measurements can also validate the accuracy and effectiveness of the proposed robust TVPI method.

3) Comparison of SLM and CLM: Fig. 8 compares the measured and estimated active power using three methods and SLM/CLM models. As can be seen, the active power profile using any method on SLM shows a better fit of measured active power than that using CLM. When using Method 3 on CLM, there is a largest difference between measured and estimated active power. This is mainly caused by the equivalent impedance which makes the dynamics of equivalent IM model differ from that of the actual IM in distribution networks. The difference of active power in Fig. 8 is mainly consumed on the resistance of the equivalent impedance.

B. 129-Bus Distribution Network

This section shows the results on the 129-bus distribution network in which 128 buses are directly or indirectly connected to the main grid through Bus 1. In this system, there are totally 64 IM-load and 32 ZIP-load. The disturbance of

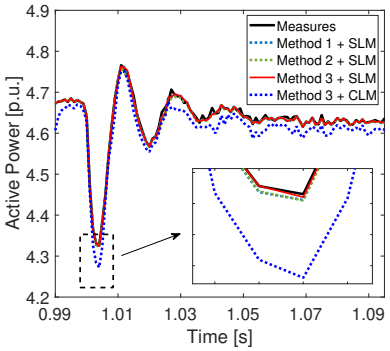

Fig. 8. Comparison of measured and estimated active power using three methods and SLM/CLM models in the 9-bus system.

voltage drop and the noise of measurement data are set the same as in the 9-bus system.

1) Effectiveness Analysis of the Proposed Method: Fig. 9 illustrates six representative parameters: $R_{s,t}$, $X_{s,t}$, $X_{r,t}$, $b_{p,t}$, $b_{q,t}$, and $\lambda_{p,t}$, which are estimated by three methods. Compared with Method 1 and Method 2, it is shown that Method 3 estimates the most accurate and robust results with the closest distance to the mean value line in blue for all time-varying parameters. Even for time points with disturbances after 1 s, it can also provide estimation results with the least influence of voltage disturbances.

Another interesting finding in Figs. 9b and 9c is that the parameter curves using Method 2 (the green dash line) significantly diverge from the blue mean value line when the voltage disturbance occurs. Under this circumstance, Method 2 performs worse than both Method 1 and Method 3. The main reason is that Method 2 does not consider the proposed robust TVPI engine. Though the advanced tolerance threshold is used in Method 2, the estimated results are still very sensitive to the voltage disturbance. Once one time point is deteriorated by the disturbance, its following time points will also be significantly misled one by one. To quantitatively evaluate the performance of Method 3, Table III shows the metrics of time-varying parameters using different methods. It can be found that Method 3 shows the smallest metrics compared with Method 1 and Method 2. We can get the same conclusion as in Table II that Method 3 can estimate not only more accurate results with smaller MAPE and RMSE but also more stable results with smaller standard deviation.

2) Robustness Analysis to Different Measurement Noises: To further validate the robustness of the developed method, Fig. 10 analyzes the impact of different measurement noises on estimated time-varying parameters by taking the stator resistance $R_{s,t}$ as an example. Metrics of standard deviation in Fig. 10a and MAPE in Fig. 10b are used for comparison. The measurement noise is increased from 0.4×10^{-3} to 4.8×10^{-3}.

In Fig. 10a, Method 3 provides the smallest standard deviation in the range of 0.8∼1.1 for the estimated parameter $R_{s,t}$ under all measurement noises. It indicates that the proposed Method 3 can estimate the most stable results compared with Method 1 and Method 2. In Fig. 10b, Method 3 provides the smallest MAPE in the range of 2%∼3% for the estimated parameter $R_{s,t}$ under all measurement noises. It indicates that

TABLE II
METRICS OF ESTIMATION METHODS IN THE 9-BUS DISTRIBUTION SYSTEM

Parameters	MAPE [%]			RMSE [%]			Standard Deviation		
	Method 1	Method 2	Method 3	Method 1	Method 2	Method 3	Method 1	Method 2	Method 3
$R_{s,t}$	4.71	5.60	**1.88**	2.17	2.43	**0.94**	1.92	2.01	**0.88**
$X_{s,t}$	1.87	1.79	**1.59**	1.16	0.67	**0.62**	1.16	0.67	**0.61**
$X_{m,t}$	8.09	3.34	**2.21**	2.45	0.96	**0.14**	1.85	0.74	**0.13**
$R_{r,t}$	2.31	2.32	**0.51**	1.04	1.05	**0.28**	1.65	1.68	**0.76**
$X_{r,t}$	3.05	2.41	**1.95**	1.35	0.59	**0.47**	1.35	0.59	**0.46**
H_t	1.13	1.14	**0.27**	8.87	8.89	**2.39**	1.21	1.22	**0.33**
$a_{p,t}$	2.37	3.29	**1.02**	3.30	2.99	**1.09**	3.22	2.41	**1.06**
$b_{p,t}$	1.65	1.22	**0.34**	1.92	1.16	**0.38**	1.78	0.96	**0.36**
$a_{q,t}$	4.73	5.51	**2.41**	5.76	6.19	**2.93**	5.21	5.37	**2.75**
$b_{q,t}$	10.12	8.40	**2.18**	4.74	3.75	**1.18**	4.37	3.20	**1.09**
$\lambda_{p,t}$	0.36	0.37	**0.24**	0.82	0.51	**0.36**	0.81	0.43	**0.34**
$\lambda_{q,t}$	2.23	1.28	**0.89**	3.95	2.69	**1.51**	3.87	2.69	**1.44**
$R_{l,t}$	16.97	16.09	**9.74**	6.99	6.42	**4.19**	6.49	5.93	**3.99**
$X_{l,t}$	4.06	4.09	**3.27**	3.39	3.44	**2.86**	3.17	3.32	**2.73**

TABLE III
METRICS OF ESTIMATION METHODS IN 129-BUS DISTRIBUTION SYSTEM

Parameters	MAPE [%]			RMSE [%]			Standard Deviation		
	Method 1	Method 2	Method 3	Method 1	Method 2	Method 3	Method 1	Method 2	Method 3
$R_{s,t}$	10.91	11.70	**1.96**	3.87	4.03	**0.98**	2.38	2.15	**0.92**
$X_{s,t}$	2.46	18.75	**1.31**	0.56	3.46	**0.25**	0.51	2.81	**0.23**
$X_{m,t}$	2.81	1.79	**0.48**	1.07	0.67	**0.26**	1.06	0.51	**0.24**
$R_{r,t}$	4.38	4.37	**1.41**	2.08	2.09	**0.81**	4.86	4.88	**2.78**
$X_{r,t}$	5.78	23.33	**1.64**	0.91	3.55	**0.25**	0.77	2.88	**0.23**
H_t	1.99	2.02	**0.51**	1.44	1.45	**0.36**	2.78	2.75	**1.56**
$a_{p,t}$	1.04	6.35	**0.66**	0.78	4.66	**0.41**	0.78	4.32	**0.41**
$b_{p,t}$	1.48	3.91	**0.19**	1.54	4.61	**0.26**	1.53	3.62	**0.23**
$a_{q,t}$	4.63	7.32	**2.01**	4.11	6.32	**2.05**	3.97	5.89	**1.95**
$b_{q,t}$	6.25	6.93	**1.62**	4.42	4.81	**1.32**	4.03	3.77	**1.24**
$\lambda_{p,t}$	0.13	0.24	**0.09**	0.27	0.33	**0.12**	0.27	0.32	**0.12**
$\lambda_{q,t}$	1.88	4.55	**1.83**	2.61	5.93	**2.06**	2.49	5.31	**1.85**
$R_{l,t}$	5.63	11.12	**5.11**	3.14	4.87	**2.41**	3.14	4.71	**2.31**
$X_{l,t}$	2.94	4.34	**1.81**	2.86	4.35	**2.01**	2.62	3.94	**1.91**

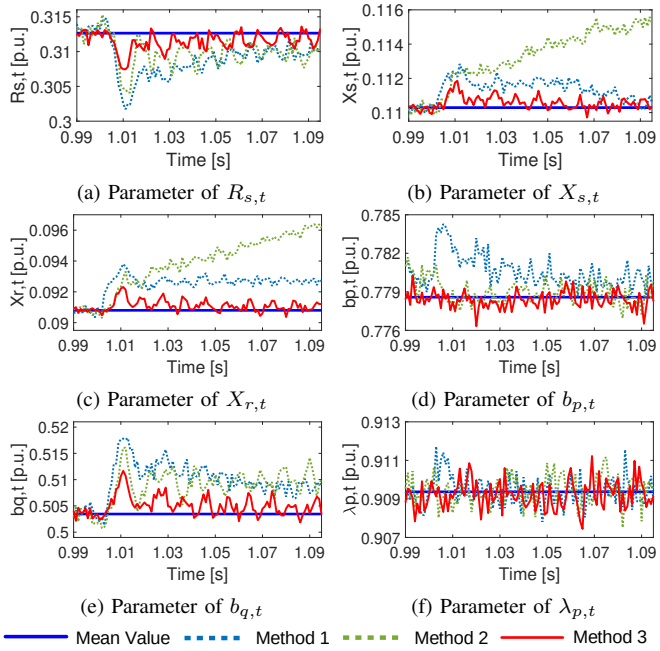

(a) Parameter of $R_{s,t}$ (b) Parameter of $X_{s,t}$

(c) Parameter of $X_{r,t}$ (d) Parameter of $b_{p,t}$

(e) Parameter of $b_{q,t}$ (f) Parameter of $\lambda_{p,t}$

Fig. 9. Six representative parameters estimated in the 129-bus system.

the proposed Method 3 can estimate the most accurate results. Overall, the TVPI results obtained by Method 3 are relatively robust to different measurement noises.

In addition, Method 2 can provide more stable results than Method 1 with smaller standard deviation as shown in Fig. 10a. However, it cannot provide more accurate results than Method 1 as shown in Fig. 10b where MAPEs of Method 2 are larger than those of Method 1. This indicates that, by just tuning the advanced tolerance thresholds, it is still challenging for Method 2 to obtain robust results. It is the developed robust TVPI engine considered in Method 3 that can significantly improve the robustness of TVPI methods.

3) Computational Time Analysis: Due to the design of a robust TVPI engine with a significantly smaller threshold η_2 for the step- and function-tolerance, more iterations are required and take longer computational time. However, the advantage of the proposed Method 3 is a trade-off between the computational time and the estimation accuracy. Table IV illustrates the numerical results of computational time and the RMSE metric of estimated parameter $X_{m,t}$. Method 1 is taken as the benchmark. As shown in this table, though the computation time is slightly increased by using Method 2 and Method 3, the RMSE metric of parameter $X_{m,t}$ is significantly reduced. For Method 2, the 11% increment of computational time can reduce RMSE by 37%. For Method 3, the 17% increment of computational time can significantly reduce RMSE by 76%. This finding can validate the benefits of the computational time increment for the proposed method.

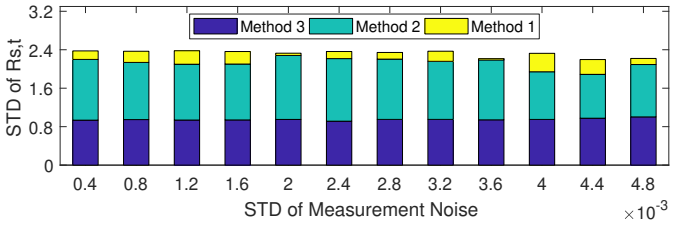

(a) Standard Deviation

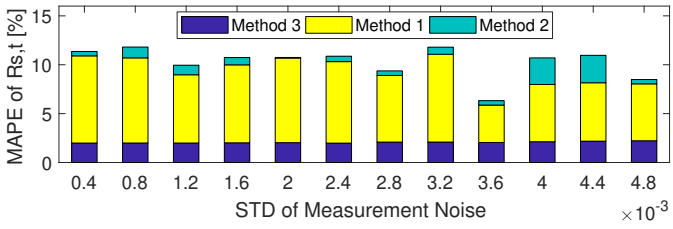

(b) MAPE

Fig. 10. Impacts of measurement noises on estimated parameter $R_{s,t}$ in the 129-bus system.

TABLE IV
COMPARISON OF COMPUTATIONAL TIME AND RMSE METRIC OF ESTIMATED PARAMETER $X_{m,t}$

Metrics	Method 1	Method 2	Method 3
RMSE [%]	1.07	0.67	0.26
Computational Time [s]	1.52	1.68	1.79
RMSE Decrement [%]	\	37	76
Computational Time Increment [%]	\	11	18

TABLE V
COMPARISON WITH/WITHOUT TIME-VARYING CHARACTERISTICS OF DYNAMIC SLM USING RMSE METRIC

Systems	Measurements	W/O [%]	With [%]
9-bus	Active Power	1.54	0.28
	Reactive Power	2.15	0.76
	Voltage	1.13	0.34
129-bus	Active Power	4.62	1.81
	Reactive Power	2.38	0.92
	Voltage	1.44	0.81

C. Impacts of Time-Varying Characteristics of Dynamic SLM

The estimated time-varying parameters in Figs. 6 and 9 in the 9- and 129-bus systems are used to compare with time-invariant parameters (i.e., constant values). Table V shows the comparison results with/without considering time-varying characteristics of dynamic SLM. The RMSE metrics of measurements (active/reactive power and voltage) are used for numerical comparison. As shown in this table, by considering the time-varying characteristics of dynamic SLM, the RMSE metrics of measurements for both simulation systems are reduced to smaller values, which means more accurate measurements can be obtained. However, when time-varying characteristics of dynamic SLM are not considered, the RMSE metrics of measurements for both simulation systems are relatively large. This observation can prove that time-varying characteristics of dynamic SLM should not be ignored for the study of load modeling.

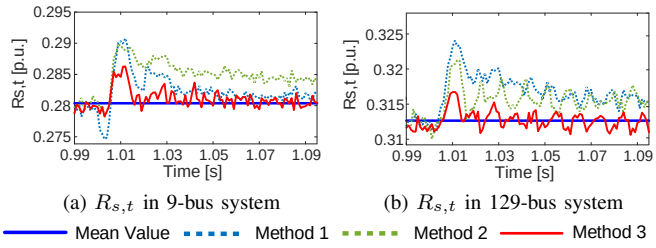

(a) $R_{s,t}$ in 9-bus system (b) $R_{s,t}$ in 129-bus system

Fig. 11. Estimated parameter $R_{s,t}$ in both 9- and 129-bus systems with a voltage increase from 1.0 p.u. to 1.1 p.u. at Bus 1.

D. Effectiveness Analysis with Voltage Increase

To further validate the effectiveness of the developed method, a bus voltage increases from 1.0 p.u. to 1.1 p.u. at Bus 1 in both 9- and 129-bus systems. The voltage increase is set at 1 second. Fig. 11 shows the estimated parameter $R_{s,t}$ as a representative in both 9- and 129-bus systems. As shown in this figure, the performance of Method 1 (the blue dash line) and Method 2 (the green dash line) is not stable and robust compared with the benchmark mean value (the blue solid line). A significant upward variation caused by the voltage increase can be seen when using Method 1 and Method 2. This is because both Method 1 and Method 2 only use the basic TVPI model where the current TVPI is highly dependent on that at the latest time point. Method 3 in the red solid curve shows the best performance compared with Method 1 and Method 2 with the closest distance to the blue solid line (the benchmark). Especially when the voltage increase occurs at 1 second, Method 3 shows the most stable results with a slightest change. This observation can validate the effectiveness of the developed method for coping with a voltage increase.

E. Effectiveness Analysis with Voltage Fall and Recovery

To show the effectiveness and adaptability of the developed method, a form of voltage disturbances with a voltage fall at 1.0 s and a voltage recovery at 1.05 s is simulated on the same structure and parameters of both 9- and 129-bus systems. Fig. 12 shows results of the estimated parameter $R_{s,t}$ as a representative in both systems. As can be seen in this figure, the performance of Method 1 (the blue dash line) and Method 2 (the green dash line) is not stable and robust compared with the benchmark mean value (the blue solid line). A significant downward fluctuation caused by the voltage fall at time 1.0 s, and a significant upward fluctuation caused by the voltage recovery at time 1.05 s can be seen when using Method 1 and Method 2. Method 3 shows the most accurate and stable results of parameter $R_{s,t}$ for both systems with the closest distance to the benchmark blue line. Especially when the voltage fall occurs at 1.0 s and the voltage recovers at 1.05 s, Method 3 shows the most stable results with the slightest changes. This finding can validate the effectiveness and adaptability of the developed method for coping with both voltage fall and recovery.

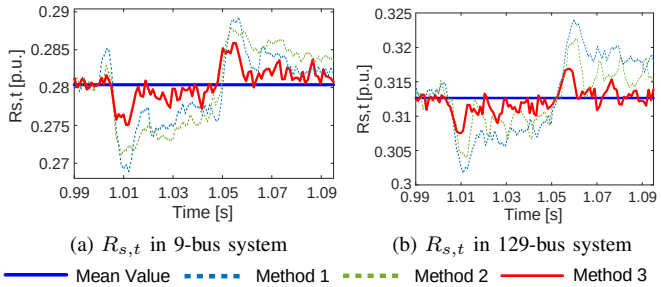

(a) $R_{s,t}$ in 9-bus system (b) $R_{s,t}$ in 129-bus system

Fig. 12. Estimated parameter $R_{s,t}$ in both 9- and 129-bus systems with a voltage fall at 1.0 s and a voltage recovery at 1.05 s.

TABLE VI
COMPARISON WITH TIME-VARYING ERM AND SLM MODEL USING RMSE METRIC

Systems	Measurements	With ERM [%]	With SLM [%]
9-bus	Active Power	0.78	0.28
	Reactive Power	1.34	0.76
	Voltage	0.85	0.34
129-bus	Active Power	2.21	1.81
	Reactive Power	1.22	0.92
	Voltage	1.18	0.81

F. Effectiveness Comparison With Exponential Recovery Model

To further validate the effectiveness of the developed method using the SLM model, the exponential recovery model (ERM) in [18] is used for comparison. Table VI shows the comparison results based on the time-varying ERM and SLM models. The RMSE metrics of measurements (active/reactive power and voltage) are used for numerical comparison. As shown in this table, when using the SLM model, the RMSE metrics of measurements for both simulation systems are slightly reduced with smaller values. This indicates that more accurate measurements can be estimated using the SLM model compared with the ERM model. This is because the exponential recovery model cannot represent different load compositions, while the SLM load model can adaptively change the time-varying percentage parameters of the Z, I, and P compositions.

V. DISCUSSION

With the recent increasing development and installation of distribution-level PMU and wave measurement devices in distribution systems, the measurement data of active power, reactive power, and voltage can be sampled in a considerably precise reporting rate, that is, 30–120 samples per second. PMU measurements make it completely possible to estimate time-varying load parameters in a small transient time interval.

To apply the estimated time-varying parameters in the small transient time interval, Fig. 13 compares the flowchart of the proposed time-varying load model with the conventional time-invariant load model. For the conventional load model, load parameters are estimated as constant values by using least square methods during the whole transient time interval. Since the parameters cannot be adaptively time-varying, the estimated measurements of active power and reactive power are less accurate. For the time-varying load model,

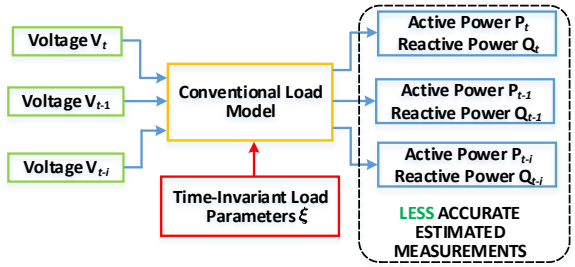

(a) Flowchart of conventional time-invariant load model

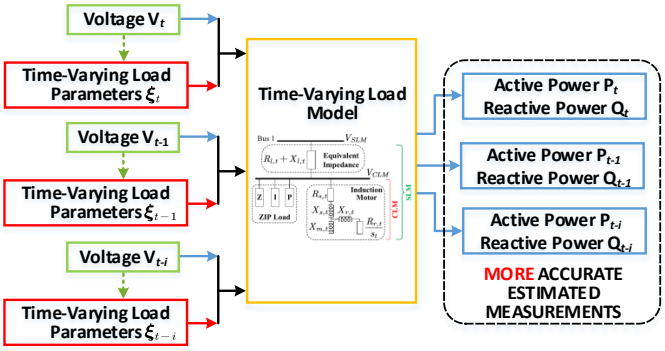

(b) Flowchart of proposed time-varying load model

Fig. 13. Comparison of the application of the proposed time-varying load model with the conventional time-invariant load model.

load parameters are adaptively estimated at each time step during the transient time interval. Consequently, the estimated measurements of active power and reactive power are more accurate compared with those using the conventional time-invariant load model.

VI. CONCLUSION

In this paper, we propose a robust time-varying parameter identification (TVPI) method in distribution networks considering voltage disturbances. The time-varying synthesis load modeling (SLM) is used with the combination of dynamic equivalent impedance, ZIP, and induction motor load. Dynamic programming is used to detect disturbances from measurement data. To cope with TVPI under voltage disturbances, a robust TVPI engine is designed and inserted into the mathematical model of time-varying SLM. The nonlinear least square (NLS) method with the trust-region-reflective algorithm is used to solve the nonlinear optimization problem. In addition, advanced tolerance thresholds are also required during iterations of NLS. Numerical simulations and comparisons of three TVPI methods show that:

(i) The proposed TVPI method can estimate more accurate and stable results of time-varying parameters with the smallest MAPE, RMSE, and standard deviations under voltage disturbances.
(ii) The estimation profile of measurement variables using SLM shows a better fit of measurement data than that using CLM. The time-varying SLM can model the dynamic load more accurately.

(iii) The proposed TVPI method is robust to different measurement noises with relatively smaller standard deviations and MAPEs of estimated parameters.

In future work, this research can be further improved by: (i) considering the three-phase unbalanced fault as a type of disturbances to further validate the effectiveness of the proposed robust time-varying parameter identification method; and (ii) analyzing the cause of parameter changes in Fig. 6 and Fig. 9, which are different from each other.

ACKNOWLEDGMENT

This work is funded by SGCC Science and Technology Program under contract no. SGSDYT00FCJS1700676. The authors would like to thank the anonymous reviewers for their constructive suggestions to this research.

REFERENCES

[1] A. Arif, Z. Wang, J. Wang, B. Mather, H. Bashualdo, and D. Zhao, "Load modeling–a review," *IEEE Trans. Smart Grid*, vol. 9, no. 6, pp. 5986–5999, Nov. 2018.

[2] C. Wang, Z. Wang, J. Wang, and D. Zhao, "Robust time-varying parameter identification for composite load modeling," *IEEE Trans. Smart Grid*, vol. 10, no. 1, pp. 967–979, Jan. 2017.

[3] E. O. Kontis, T. A. Papadopoulos, A. I. Chrysochos, and G. K. Papagiannis, "Measurement-based dynamic load modeling using the vector fitting technique," *IEEE Trans. Power Syst.*, vol. 33, no. 1, pp. 338–351, Jan. 2018.

[4] WECC Dynamic Composite Load Model (CMPLDW) Specifications. [Online]. Available: https://www.wecc.biz/Reliability/WECC%20Composite%20Load%20Model%20Specifications%2001-27-2015.docx

[5] R. He, J. Ma, and D. J. Hill, "Composite load modeling via measurement approach," *IEEE Trans. Power Syst.*, vol. 21, no. 2, pp. 663–672, May 2006.

[6] J. Ma, R. He, and D. J. Hill, "Load modeling by finding support vectors of load data from field measurements," *IEEE Trans. Power Syst.*, vol. 21, no. 2, pp. 726–735, May 2006.

[7] Y. Pang, Y. Xu, and S. Tao, "A study on the load model based on particle swarm optimization," in *2016 IEEE 11th Conference on Industrial Electronics and Applications (ICIEA)*, Hefei, China, Jun. 596–601, 2016.

[8] P. Ju, K. Shi, Y. Tang, Z. Shao, Q. Chen, and W. Yang, "Comparisons between the load models with considering distribution network directly or indirectly," in *2008 Joint International Conference on Power System Technology and IEEE Power India Conference*, New Delhi, India, Oct. 12–15, 2008.

[9] I. A. Hiskens, "Nonlinear dynamic model evaluation from disturbance measurements," *IEEE Trans. Power Syst.*, vol. 16, no. 4, pp. 702–710, Nov. 2001.

[10] J. Zhao, M. Netto, and L. Mili, "A robust iterated extended Kalman filter for power system dynamic state estimation," *IEEE Trans. Power Syst.*, vol. 32, no. 4, pp. 3205–3216, Jul. 2017.

[11] J. De Kock, F. Van Der Merwe, and H. Vermeulen, "Induction motor parameter estimation through an output error technique," *IEEE Trans. Energy Convers.*, vol. 9, no. 1, pp. 69–76, Mar. 1994.

[12] T. Hiyama, M. Tokieda, W. Hubbi, and H. Andou, "Artificial neural network based dynamic load modeling," *IEEE Trans. Power Syst.*, vol. 12, no. 4, pp. 1576–1583, Nov. 1997.

[13] B.-Y. Ku, R. J. Thomas, C.-Y. Chiou, and C.-J. Lin, "Power system dynamic load modeling using artificial neural networks," *IEEE Trans. Power Syst.*, vol. 9, no. 4, pp. 1868–1874, Nov. 1994.

[14] V. Knyazkin, C. A. Canizares, and L. H. Soder, "On the parameter estimation and modeling of aggregate power system loads," *IEEE Trans. Power Syst.*, vol. 19, no. 2, pp. 1023–1031, May 2004.

[15] J. Zhao, Z. Wang, and J. Wang, "Robust time-varying load modeling for conservation voltage reduction assessment," *IEEE Trans. Smart Grid*, vol. 9, no. 4, pp. 3304–3312, Jul. 2018.

[16] D. Q. Hung, N. Mithulananthan, and K. Y. Lee, "Determining PV penetration for distribution systems with time-varying load models," *IEEE Trans. Power Syst.*, vol. 29, no. 6, pp. 3048–3057, Nov. 2014.

[17] Z. Wang and J. Wang, "Time-varying stochastic assessment of conservation voltage reduction based on load modeling," *IEEE Trans. Power Syst.*, vol. 29, no. 5, pp. 2321–2328, Sep. 2014.

[18] D. J. Hill, "Nonlinear dynamic load models with recovery for voltage stability studies," *IEEE Trans. Power Syst.*, vol. 8, no. 1, pp. 166–176, Feb. 1993.

[19] J. Ma, D. Han, R.-M. He, Z.-Y. Dong, and D. J. Hill, "Reducing identified parameters of measurement-based composite load model," *IEEE Trans. Power Syst.*, vol. 23, no. 1, pp. 76–83, Feb. 2008.

[20] D. Han, J. Ma, R.-M. He, and Z.-Y. Dong, "A real application of measurement-based load modeling in large-scale power grids and its validation," *IEEE Trans. Power Syst.*, vol. 24, no. 4, pp. 1756–1764, Nov. 2009.

[21] B.-K. Choi and H.-D. Chiang, "Multiple solutions and plateau phenomenon in measurement-based load model development: issues and suggestions," *IEEE Trans. Power Syst.*, vol. 24, no. 2, pp. 824–831, May 2009.

[22] H. Bai, P. Zhang, and V. Ajjarapu, "A novel parameter identification approach via hybrid learning for aggregate load modeling," *IEEE Trans. Power Syst.*, vol. 24, no. 3, pp. 1145–1154, Aug. 2009.

[23] Y. Ge, A. J. Flueck, D.-K. Kim, J.-B. Ahn, J.-D. Lee, and D.-Y. Kwon, "An event-oriented method for online load modeling based on synchrophasor data," *IEEE Trans. Smart Grid*, vol. 6, no. 4, pp. 2060–2068, Jul. 2015.

[24] J.-K. Kim, K. An, J. Ma, J. Shin, K.-B. Song, J.-D. Park, J.-W. Park, and K. Hur, "Fast and reliable estimation of composite load model parameters using analytical similarity of parameter sensitivity," *IEEE Trans. Power Syst.*, vol. 31, no. 1, pp. 663–671, Jan. 2016.

[25] C. Wang, Z. Wang, J. Wang, and D. Zhao, "SVM-based parameter identification for composite ZIP and electronic load modeling," *IEEE Trans. Power Syst.*, vol. 34, no. 1, pp. 182–193, Jan. 2019.

[26] Y. Wang, Q. Chen, T. Hong, and C. Kang, "Review of smart meter data analytics: Applications, methodologies, and challenges," *IEEE Trans. Smart Grid*, vol. 10, no. 3, pp. 3125–3148, May 2019.

[27] Y. Wang, N. Zhang, Q. Chen, D. S. Kirschen, P. Li, and Q. Xia, "Data-driven probabilistic net load forecasting with high penetration of behind-the-meter PV," *IEEE Trans. Power Syst.*, vol. 33, no. 3, pp. 3255–3264, May 2018.

[28] L. Zhou, Z. W. Peng, C. R. Deng, X. Z. Qi, and P. Q. Li, "A generalized synthesis load model considering network parameters and all-vanadium redox flow battery," *Protection and Control of Modern Power Systems*, vol. 3, no. 3, pp. 315–327, Oct. 2018.

[29] The Mathworks, Inc. Nonlinear least square solver. [Online]. Available: https://www.mathworks.com/help/optim/ug/lsqnonlin.html.

[30] D.-I. Kim, T. Y. Chun, S.-H. Yoon, G. Lee, and Y.-J. Shin, "Wavelet-based event detection method using PMU data," *IEEE Trans. Smart Grid*, vol. 8, no. 3, pp. 1154–1162, May 2017.

[31] M. K. Jena, B. K. Panigrahi, and S. R. Samantaray, "A new approach to power system disturbance assessment using wide-area postdisturbance records," *IEEE Trans. Ind. Inform.*, vol. 14, no. 3, pp. 1253–1261, Mar. 2018.

[32] L. Xie, Y. Chen, and P. R. Kumar, "Dimensionality reduction of synchrophasor data for early event detection: Linearized analysis," *IEEE Trans. Power Syst.*, vol. 29, no. 6, pp. 2784–2794, Nov. 2014.

[33] M. Cui, J. Wang, J. Tan, A. Florita, and Y. Zhang, "A novel event detection method using PMU data with high precision," *IEEE Trans. Power Syst.*, vol. 34, no. 1, pp. 454–466, Jan. 2019.

[34] N. G. Boulaxis and M. P. Papadopoulos, "Optimal feeder routing in distribution system planning using dynamic programming technique and GIS facilities," *IEEE Trans. Power Deliv.*, vol. 17, no. 1, pp. 242–247, Jan. 2002.

[35] M. Cui, D. Ke, Y. Sun, D. Gan, J. Zhang, and B.-M. Hodge, "Wind power ramp event forecasting using a stochastic scenario generation method," *IEEE Trans. Sustain. Energy*, vol. 6, no. 2, pp. 422–433, Apr. 2015.

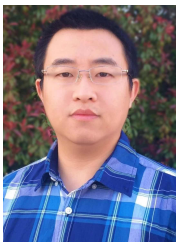

Mingjian Cui (S'12–M'16–SM'18) received the B.S. and Ph.D. degrees from Wuhan University, Wuhan, Hubei, China, all in Electrical Engineering and Automation, in 2010 and 2015, respectively.

Currently, he is a Research Assistant Professor at Southern Methodist University, Dallas, Texas, USA. He was also a Visiting Scholar from 2014 to 2015 in the Transmission and Grid Integration Group at the National Renewable Energy Laboratory (NREL), Golden, Colorado, USA. His research interests include renewable energy, smart grid, machine learning, data analytics, power system operation, PMU, optimization modeling, electricity market, cybersecurity, and load modeling. He has authored/coauthored over 50 peer-reviewed publications. Dr. Cui serves as an Associate Editor for the journal of IET Smart Grid. He is also the Best Reviewer of the IEEE Transactions on Smart Grid for 2018.

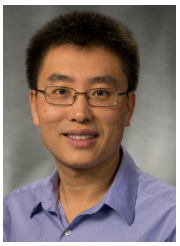

Jianhui Wang (M'07–SM'12) received the Ph.D. degree in electrical engineering from Illinois Institute of Technology, Chicago, Illinois, USA, in 2007.

Presently, he is an Associate Professor with the Department of Electrical Engineering at Southern Methodist University, Dallas, Texas, USA. Prior to joining SMU, Dr. Wang had an eleven-year stint at Argonne National Laboratory with the last appointment as Section Lead – Advanced Grid Modeling. Dr. Wang is the secretary of the IEEE Power & Energy Society (PES) Power System Operations, Planning & Economics Committee. He has held visiting positions in Europe, Australia and Hong Kong including a VELUX Visiting Professorship at the Technical University of Denmark (DTU). Dr. Wang is the Editor-in-Chief of the IEEE Transactions on Smart Grid and an IEEE PES Distinguished Lecturer. He is also a Clarivate Analytics highly cited researcher for 2018.

Yishen Wang (S'13–M'17) received the B.S. degree in electrical engineering from Tsinghua University, Beijing, China, in 2011, the M.S. and the Ph.D. degree in electrical engineering from the University of Washington, Seattle, WA, USA, in 2013 and 2017, respectively. He is currently a Power System Research Engineer with GEIRI North America, San Jose, CA, USA. His research interests include power system economics and operation, energy storage, microgrids, load modeling and PMU data analytics.

Ruisheng Diao (M'09–SM'15) obtained his Ph.D. degree in EE from Arizona State University, Tempe, AZ, in 2009. Serving as a project manager, PI/co-PI and key technical contributor, Dr. Diao has been managing and supporting a portfolio of research projects in the area of power system modeling, dynamic simulation, online security assessment and control, dynamic state estimation, integration of renewable energy, and HPC implementation in power grid studies. He is now with GEIRINA as deputy department head, AI & System Analytics, in charge of several R&D projects on power grid high-fidelity simulation tools and developing new AI methods for grid operations.

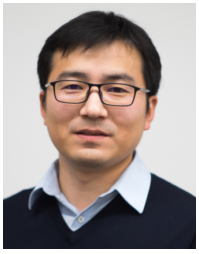

Di Shi (M'12–SM'17) received the B. S. degree in electrical engineering from Xi'an Jiaotong University, Xian, China, in 2007, and M.S. and Ph.D. degrees in electrical engineering from Arizona State University, Tempe, AZ, USA, in 2009 and 2012, respectively. He currently leads the AI & System Analytics Group at GEIRI North America, San Jose, CA, USA. His research interests include WAMS, energy storage systems, and renewable integration. He is an Editor of IEEE Transactions on Smart Grid and IEEE Power Engineering Letters.